REACTIONS IN SOLID PHASE—II

KARTAR SINGH

Defence Science Laboratory, Delhi

(*Received* 23 *February*, 1966)

The production of oxide film capacitors and protective coatings on metals involves controlled oxidation of metals. The reactions which may give homogeneous, dense and coherent films on oxidation of metals and semiconductors have been discussed in this paper. The present position regarding mechanisms of oxidation in space charge regions and in field free regions has been presented. The factors which control the rate of oxidation have been highlighted.

In the first part chemical reactivity in solids has been discussed. Oxidation of metals is another important topic in this field. In the production of new materials; pyrotechnics; ammunition; new electronic devices including capacitors, rectifiers and resistors, a knowledge about the oxidation of metals is of immense importance.

In the development of high temperature materials, 'temperature capability' is an important quality. It may be defined as the maximum temperature at which materials can resist a load of 20,000 lbs. p.s.i. for 100 hours. The critical property in high temperature application may not be melting point or even strength at high temperature. It may lie instead in oxidation resistance. Most successful coatings for imparting oxidation resistance are formed by vapour phase impregnation. Vapours of silicon, titanium or zirconium are allowed to diffuse. The diffused metal is subjected to controlled oxidation to form a metal bonded or metal modified oxide coating.

For about half a century anodic oxidation of metals such as aluminium, tantalum or silicon has been extensively used in the production of capacitors. Micro-circuitry based upon thin film oxide capacitors or resistors offer a new promise in the field of electronics. Thin oxide film on silicon has been extensively used in planar technology for masking the diffusion of impurities.

One of the important properties of oxide film which influences the mechanism of oxidation is the molar volume V. If V (compound) $> V$ (metal), the oxide film is dense and coherent. If V (compound) $< V$ (metal), the oxide film shows cracks and sponginess. A progressive increase in film thickness influences the mechanism of oxidation. The demarcation between thick and thin films lies at about 1000 A. For thin films one of the following laws may be applicable

$$x^3 = k_c\, t \tag{1}$$

$$x = k_u \left(\log \frac{t}{\tau} + 1\right) \tag{2}$$

$$\frac{1}{x} = k_{i1} - k_{i2} \log t \tag{3}$$

where x is thickness of the oxide, t is time, τ, k_c, k_u, k_{i1} and k_{i2} are constants. These laws can be derived by taking account of effects of electric field and space charge. In case of thick layers one of the following two laws may be applicable

$$x = Bt \quad \text{Linear law,} \tag{4}$$

$$x^2 = 2At \quad \text{(Parabolic law)} \tag{5}$$

where A and B are constants.

The linear law may be followed when reaction at one of the inter-faces is slow. As for example the rate of oxidation of iron in an atmosphere of carbon dioxide is dependent upon the slow reaction

$$CO_2 \rightarrow \bar{O}\,(a) + h^+ + CO \tag{6}$$

which occurs at the oxide/gas inter-face. Here $h+$ is a hole in the full valence band, and subscript (a) indicates 'adsorbed'. The parabolic law can be derived on the basis of migration of defects under the combined influence of concentration gradient and diffusion potential.

The initial step in the oxidation process is the adsorption of oxygen. The mass (m_g) of the gas which strikes against the unit surface of the metal per second is given by the expression

$$m_g = \frac{1}{4}\,\zeta\,\rho \tag{7}$$

where $\frac{1}{2}\,\zeta$ is average component of velocity in the given direction, $\frac{1}{2}\,\rho$ is mass per unit volume which is moving towards the metal. Assuming the gas law

$$\rho = \frac{PM}{RT}$$

and the result of the kinetic theory

$$\zeta = \sqrt{\frac{8RT}{\pi M_g}}$$

expression (7) assumes the form

$$m_g = (M_g/2\pi RT)^{\frac{1}{2}} \cdot P \tag{8}$$

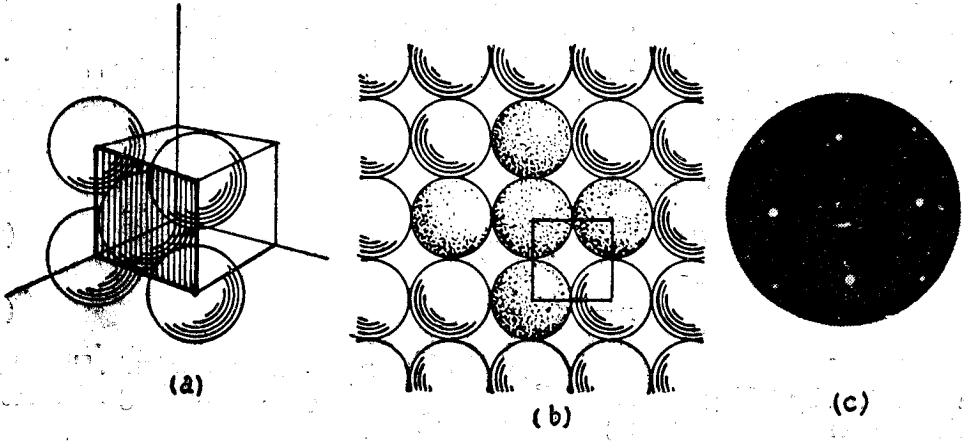

FIG. 1—(a) Geometry of (100) face of nickel, (b) atomic arrangement on (100) face of nickel and (c) electron diffraction pattern of (100) face of nickel

where M_g is molecular weight of the gas, R is gas contstant, T is temperature in degrees absolute and P is pressure of the gas. The number (n_g) of gas molecules striking the surface is given by the expression

$$n_g = (1/2\pi M_g RT)^{\frac{1}{2}} . P \qquad (9)$$

The rate (J_g) at which the molecules are physically adsorbed on the surface is given by the expression

$$J_g = \epsilon_a P(O_2)/(2\pi M_g RT)^{\frac{1}{2}} \qquad (10)$$

where ϵ_a is the probability that a molecule striking the surface will stick. Sticking coefficient may be attributed to decrease in entropy. Hindered rotation of the molecule in chemisorbed state reduces the coefficient below unity.

$$\epsilon_a = \sigma_s \; h^2/8\pi^2 I kT$$

where h is Planck's constant, I is moment of inertia, k is Boltzmann' constant and σ_s is symmetry factor.

Mechanism of initial uptake of oxygen is revealed by the study of low energy electron diffraction[1]. As for example adsorption of oxygen on nickel surface produces a striking change in its diffraction pattern. A comparison of Fig. 1*c* and 4*b* shows that on adsorption of oxygen at its clean (100) surface the diffraction order is reduced to half in both directions. The change occurs at a coverage of $\theta = 0 \cdot 25$. The atomic arrangements at (100), (110) and (111) faces of a face centred cubic crystal of nickel are shown in Fig. 1*a*, 1*b*, 2*a*, 2*b*, 3*a* and 3*b* respectively. The corresponding diffraction patterns are shown in Fig. 1*c*, 2*c* and 3*c*. On adsorption of oxygen, atoms on (100) face acquire the arrangement shown in Fig. 4*a*. It consists of a square arrays of atoms of nickel and oxygen with a cell size double that of the original. The new arrangement may be responsible for a change in diffraction pattern. Tungsten has a body centred cubic structure. The clean surface of (110) face possesses atomic arrangement shown in Fig. 5*a* and yields a diffraction pattern given in Fig. 5*b*. On adsorption of oxygen the pattern changes to the one shown in Fig. 6*b*. A possible arrangement of atoms which may give this pattern is shown in Fig. 6*a*. Adsorption of iodine[2] at (100) surface of silicon produces a pattern with third order.

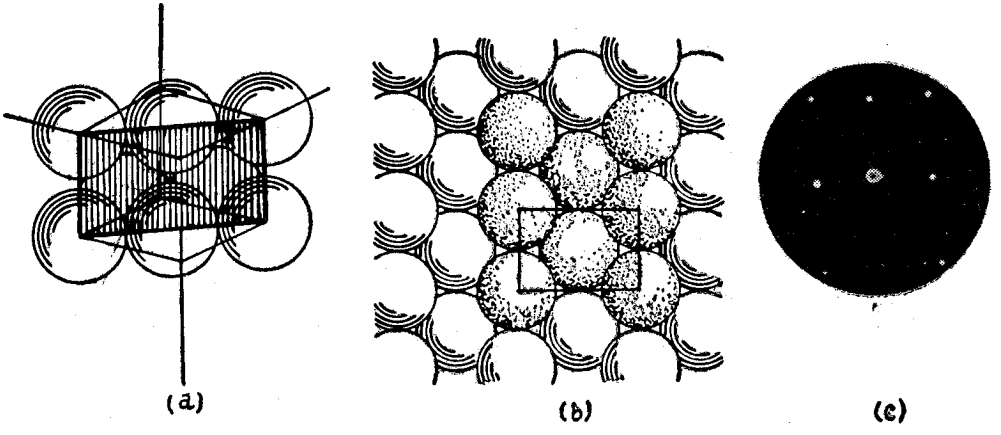

FIG. 2—(*a*) Geometry of (110) face of nickel, (*b*) atomic arrangement on (110) face of nickel and (*c*) electron diffraction pattern of (110) face of nickel

Much speculation exists regarding the exact nature of chemisorbed ions. It may[3—5] exist in one of the three forms $\bar{O}_2$, $\bar{O}$ or O^{-2}. Winter's experiments on isotope equilibrium reaction of oxygen on NiO or MgO surfaces suggest[6,7] that its adsorption is in the form $\bar{O}$ (a) ions. The isotopic equilibrium may be written in the form

$$16O_2 + 18O_2 \underset{-4e}{\overset{4e}{\rightleftharpoons}} 2\,^{16}\bar{O}\,(a) + 2^{18}\bar{O}\,(a) \underset{+4e}{\overset{-4e}{\rightleftharpoons}} 2\,^{16}O\,^{18}O \qquad (11)$$

For the dissociation to occur it is necessary to have two cation sites in close proximity. It is appropriate here to suggest that an anion vacancy may expose an adjacent

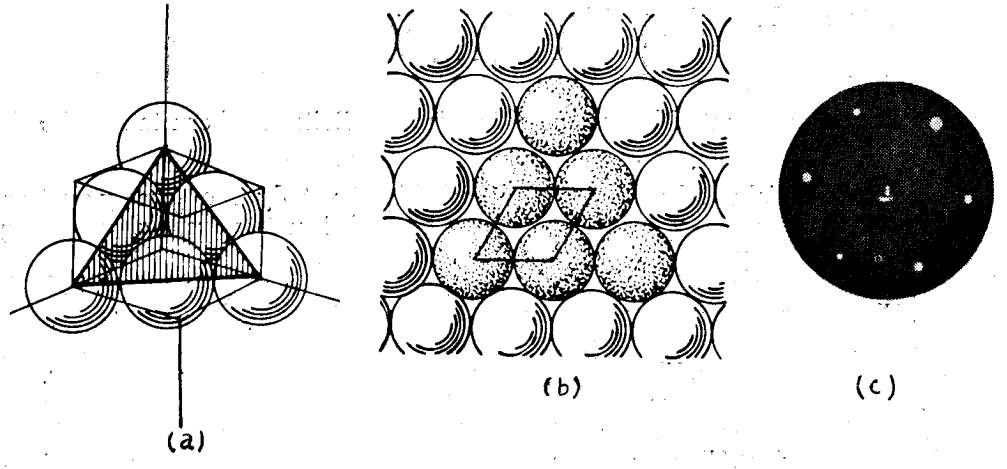

FIG. 3—(*a*) Geometry of (111) face of nickel, (*b*) atomic arrangement of (111) face of nickel and (*c*) electro diffraction pattern of (111) face of nickel

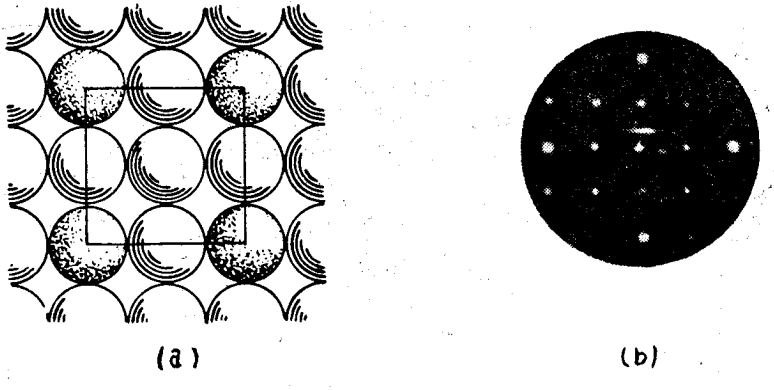

FIG. 4—(*a*) Atomic arrangement on (100) face of nickel with adsorbed exygen and (*b*) electron diffraction pattern of (100) face of nickel with adsorbed oxygen on nickel

pair of cations which may serve as adsorption centres. In case of nickel oxide[8] mechanism may be written in the form

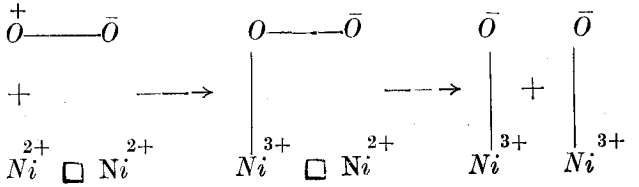

(12)

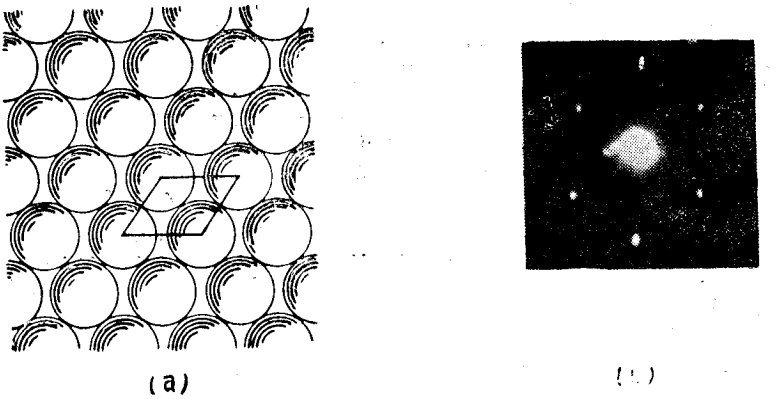

FIG. 5—(*a*) Atomic arrangement on (110) face of tungsten and (*b*) electron diffraction pattern of (110) face of tungsten

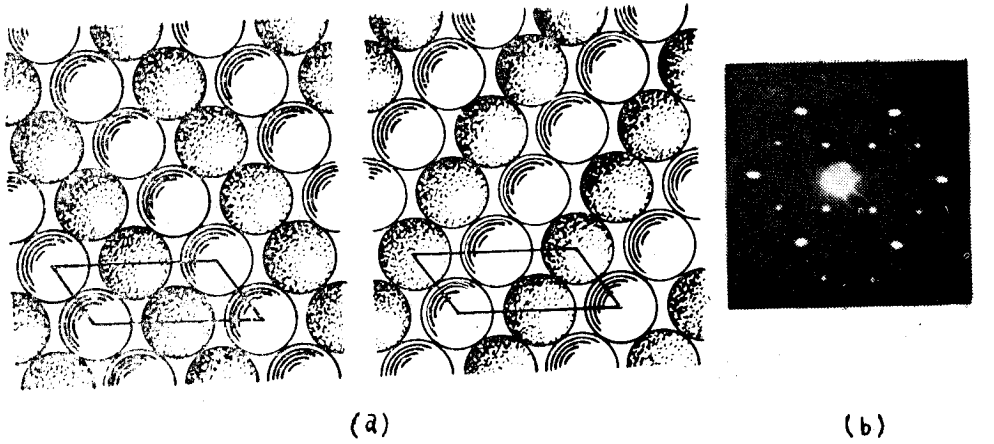

FIG. 6—(*a*) Atomic arrangement on(110) face with adsorbed oxygen and (*b*) electron diffraction pattern of (110) face of tungsten

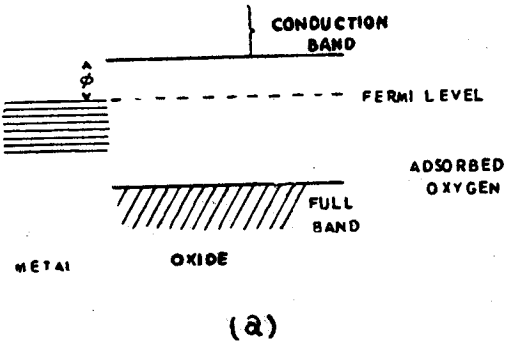

FIG. 7 (*a*)—Metal in contact with insulating oxide

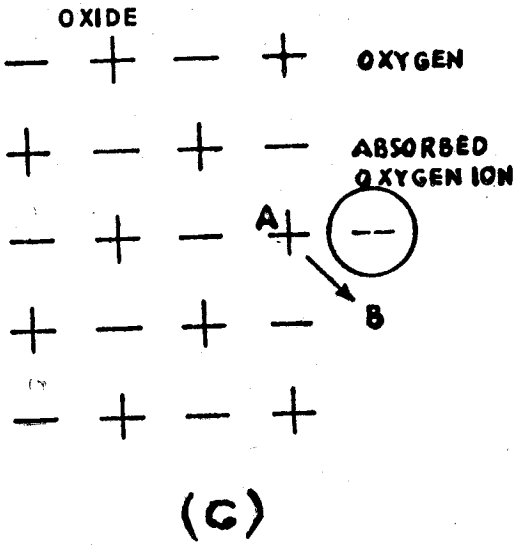

FIG. 7 (*c*)—The process by which a cation site is created in the vicinity of an absorbed oxygen ion

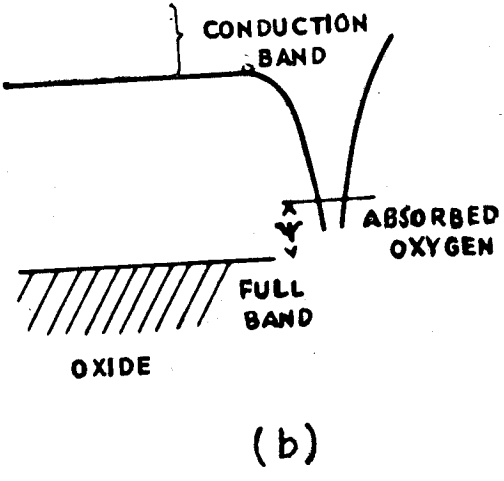

FIG. 7 (*b*)—Insulating oxide in contact with oxygen

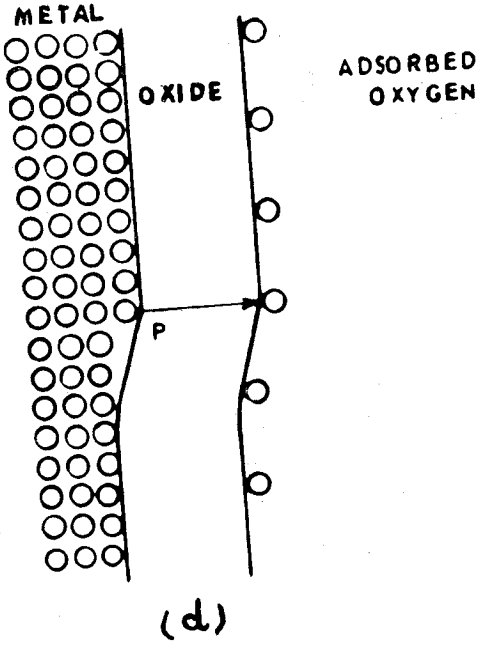

FIG. 7 (*d*)—Showing the mechanism by which ions from surface of a metal pass into oxide layers

At high temperature adsorbed oxygen may be incorporated in the surface layers of the oxide by outwards diffusion of the cations from the sites below the adsorbed oxygen as shown in Fig. 7*c*. The basic process which is responsible for oxidation is the transfer of an electron from crystal lattice of the oxide to the adsorbed oxygen atom. As a consequence of this, a hole is injected into the valence band. The electro-negativity is maintained by the formation of cation vacancy. In the case of Cu_2O the mechanism may be represented by means of the equations

$$\left.\begin{aligned} O_2 &\rightleftharpoons 2\,\bar{\bar{O}} + 4\overset{+}{h} + 4\ \square_{cu+} \\ \text{or}\quad O_2 &\rightleftharpoons 2\,\bar{\bar{O}} + (s)\ \overset{+}{h} + (s)\ \square_{cu+} \end{aligned}\right\} \qquad (13)$$

The concentrations of holes (n_h) and a cation vacancy $n_{\square}$ are given by the expressions

$$n_h{}^{+}(0) = N_e \left(\frac{N_\circ}{N_s}\right) e^{-\psi/kT} \qquad (14)$$

$$n_{\square}(0) = N_M (N_s\, a^2)\ e^{-W_{\square}/kT} \qquad (15)$$

where ψ is the energy required to excite an electron from the oxide into the adsorbed oxygen, $W_{\square}$ is the energy required for the formation of cation vacancy near adsorbed oxygen $Ne = \left(\frac{2\pi m\ kT}{h^2}\right)^{3/2}$, m is mass of electron, N_M is number of metal ion sites, 'a' is distance between ions, factor ($N_s\ a^2$) accounts for the fact that only ($N_s\ a^2$) portion out of the unit area is occupied by chemisorbed oxygen, factor ($N_\circ/N_s$) arises from the various ways in which N_s occupied levels can be distributed among the total ($N_\circ + N_s$) levels and symbol (o) signifies the location at the interface.

At the oxide/gas interface fresh molecules are adsorbed. They dissociate into atoms and entrap electrons. The cations near these sites migrate to the surface. At the metal/oxide interface electrons and cations are injected into the oxide. At the equilibrium the sum of changes in free energy for all these processes is zero. On these assumptions, the concentration of carriers within the oxide can be calculated. Well within the lattice the concentrations of holes (n_h) and vacancies $n_{\square}$ are equal. The value of $n = \sqrt{n_h . n_{\square}}$ is given by the expression[9]

$$n = \sqrt{N_e\ N_M}.\quad \left(\frac{n_g}{N_g}\right)^{\frac{1}{2s}} \exp\ \frac{-E}{2skT} \qquad (16)$$

where $N_g = (2\pi M_g\, kT/h^2)^{3/2}$ and E is the energy required for adsorption of one molecule of oxygen and formation of s cation vacancies and s holes ($s = 4$ in Cu_2O). Application of law of mass action gives the condition

$$n_h{}^{+}(0)\ n_{\square}(0) = n^2 \qquad (17)$$

By making use of (14), (15), (16) and (17), it is possible to derive the proportion of oxide area covered by adsorbed oxygen.

$$(N_\circ\, a^2) = \left(\frac{n_g}{N_g}\right)^{1/s} \exp - \left(\frac{E}{s} - \psi - W\right) \Big/ kT \qquad (18)$$

If conditions are suitable chemisorption of oxygen may lead to oxidation of the metal. The mechanism can be illustrated by considering the example of oxidation of magnesium[10] at 500°—590°C.

The reaction between oxygen and magnesium occurs according to equations

$$Mg + \tfrac{1}{2}\ O_2 \rightleftharpoons MgO$$

and

$$\left(\frac{dw}{dt}\right) / S = k_{mg}\ . P^{0\cdot5} \qquad (19)$$

where (dw/dt) is rate of increase in weight on oxidation, S is number of adsorption sites at the oxide surface and k_{mg} is rate constant. The value of $(dw/dt)/S$ as $\triangle w \rightarrow O$ can be used to derive $(k_{mg})_o$ at various temperatures. Based upon these data, activation energy is found to be 48k calories per mole. Pressure index of 1/2 in (19) indicates that atomic oxygen takes part in the reaction. The existence of acceleratory stage in oxidation implies that diffusion is not rate determining step. This is so because a diffusion controlled reaction is inversely proportional to extent of reaction. The mechanism of reaction possibly involves dissociative adsorption of oxygen, capture of electron by atomic oxygen and generation of holes in the lattice, diffusion of oxygen ions and holes through the lattice, capture of holes by oxygen ions at oxide/metal surface and reaction between atomic oxygen and magnesium at metal surface.

The adsoprtion of oxygen on S sites is given by the expression

$$\tfrac{1}{2}\ O_2\,(g) + \tfrac{1}{2}\ S \underset{km_2}{\overset{km_1}{\rightleftharpoons}} \tfrac{1}{2}\ O_2\,(a)\ S \qquad (20)$$

where symbol (g) signifies gaseous state, the ratio km_r of reaction constants km_1 and km_2 is given by the expression

$$km_r = \frac{km_1}{km_2} = \left(\frac{f_1^*\ (O_2)_a}{f\ (O_2)_g}\right)^{1/2} \exp\ \frac{-E_a}{2kT} \qquad (21)$$

where f_1^* and f are partition functions of activated complex and reactant respectively and E_a is activation energy for adsorption of oxygen. The dissociation of oxygen may be written in the form

$$\tfrac{1}{2}\ O_2\,(a)\ S \underset{km_4}{\overset{km_3}{\rightleftharpoons}} O\ (a)\ S \qquad (22)$$

and

$$km_3 = \left(\frac{kT}{h}\right)^{1/2} \left(\frac{f_2^*\ (O_2)_a}{f\ (O_2)_a}\right)^{1/2} \exp\ \frac{-E_b}{2kT} \qquad (23)$$

where E_b is energy of activation for break up of adsorbed oxygen into atoms. The rate of reaction at the oxide/metal interface may be repesented by the equations

$$Mg\ (s) + (O)_o \xrightarrow{km_5} MgO\ (s)$$

$$\frac{d\ (Mg\ O)}{dt} = km_5\ S\ \Big[\ O\ \Big]_o \qquad (24)$$

where $[O]_o$ is concentration of oxygen atoms on the oxide/metal interface and symbol (s) signifies solid state.

The concentration $(O)_o$ can be derived by making use of the steady state conditions

$$\frac{d\,[O]_o}{dt} = km_3\left[\ O_2\ \right]_a^{1/2} - km_4\left[\ O\ \right]_a - km_5\left[\ O\ \right]_a S = 0 \qquad (25)$$

$$\frac{d\,[O_2]_a}{dt} = km_1 S\left[O_2\right]_g^{1/2} + km_4\left[O\right]_a - km_2\left[O_2\right]_a^{1/2} - km_3\left[O_2\right]_a^{1/2} = 0 \qquad (26)$$

$$\text{and} \qquad [O]_o = [O]_a \qquad (27)$$

and may be represented in the form

$$\left[\ O\ \right]_a = \frac{km_r \,.\, km_3}{km_5}\left[\ O_2\ \right]_g^{1/2} \qquad (28)$$

Condition (27) follows from the fact that diffusion into the oxide film is rapid. On substituting the values of km_r, km_3, and $[O]_o$ given by (21), (23) and (28) in (24), the rate of oxidation is found to be

$$\frac{d\,(Mg\ O)}{dt} = S\cdot\left[O_2\ \right]_g^{1/2}\left(\frac{kT}{h}\right)^{1/2}\left[\frac{f_1^*\,(O_2)_a f_2^*\,(O_2)_a}{f(O_2)_g\ f(O_2)_o}\right]^{1/2}\exp-\frac{(E_a+E_b)}{kT} \qquad (29)$$

Adsorbed oxygen $(O_2)_a$ loses one translational and one rotational degree of freedom. It acquires one vibrational degree of freedom. During dissociation the vibrational degree of freedom of the oxygen molecule passes into translation. The partition functions of the adsorbed state and excited adsorbed state are related to the other as given below:

$$\left[\frac{f^*\,(O_2)_a}{f\,(O_2)_a}\right]^{1/2} = \left(1-\exp\frac{-h\nu}{kT}\right)^{1/2} = \left[\frac{h\nu}{kT}\right]^{1/2} \qquad (30)$$

On assuming $S \simeq 10^{15}$ Mg sites /cm^2 at metal oxide/oxygen interface, $[O_2]_g \simeq 9\times10^{18}$ molecules of O_2/cm^3, $T = 843°k$, $\nu \simeq 10^{13}$ and $\frac{E_a+E_b}{2} = 48$k calories/mole, the rate of reaction is found to be $\frac{d\,MgO}{dt} = 10^{16}$ of atoms of oxygen/cm^2 sec compared to experimental value of 2×10^{15} atoms of oxygen/cm^2 sec. The agreement is fairly close[10].

In majority of cases, thickness of the coherent oxide film influences the rate of oxidation. Within this film the rate determining step in oxidation may, either be entry of cation into oxide film which is brought about by field set up by tunnelling of the electrons from metal to adsorbed oxygen or emission of electrons from metal surface into oxide film with cations following them. Mott & Cabrera's[11] mechanism is based upon first assumption. Uhlig [12,13] makes use of the second assumption. According to his theory, observed[14] differences in oxidation rate of various faces of a metal may be correlated with reductions in electronic work function. Well within thick films positive and negative charges are balanced. The rate of growth in neutral layer depends mainly on diffusion. These mechanims of oxidation are discussed below :

Mott & Cabrera theory of thin film

Initially oxygen is chemisorbed on the surface of the thin film of the oxide. A field (F) is set up due to contact potential (V) of the adsorbed oxygen which has captured electron. The mechanisms of migration of electron from the metal surface to the oxide and from oxide to adsorbed oxygen are given in Fig. 7(a) and 7(b). The subsequent step is the formation of a vacancy beneath the adsorbed oxygen. The process by which a vacant site is created in the vicinity of an adsorbed oxygen ion is shown in Fig 7(c). The vacancy

diffuses through the oxide to the interface between oxide and metal. The cation moves to the vacant site as shown in Fig. 7(*d*). The motion of the cation at the metal surface located at a favourable site P takes place with activation energy E_f

$$E_f = H + U - \triangle H + \epsilon_{\square}''_0 - qa' F \tag{31}$$

where H is energy barrier for moving a cation from point P to point Q at the interface of the oxide, U is the energy required for motion of the ion in the period field of the lattice, $\triangle H$ is heat of chemisorption of oxygen, $\epsilon_{\square}''_0$ is enthalpy of the formation of anion vacancy, q is electronic charge on the ion, a' is distance PS in Figure 8. $F = \frac{V}{X}$ is field, X is film thickness.

$\triangle H$ may be taken equal to $\epsilon_{\square}''_0$. The chance (Γ) per unit time that an atom at P will escape over energy barrier located at S_1 and reach a position Q_1 is given by the expression

$$\Gamma = \nu \exp \frac{-W_c}{kT} \exp \frac{q a' F}{kT} \tag{32}$$

where ν is vibration frequency and $W_c = H + U$. The rate of growth of the film may be written in the form

$$\frac{dx}{dt} = N' \Omega \nu \exp \frac{-\left(W_c - qa' \frac{V}{X}\right)}{kT} \tag{33}$$

where N' is number of kink sites such as P on the surface of the metal, Ω is volume of oxide per cation. The critical temperature T_c below which the rate of oxidation reaches a limiting low value $(dx/dt)_L$ can be derived by making use of (33) which may be written in the form

$$\frac{kT}{W}\left[\log \left(\frac{dx}{dt}\right)_L \frac{1}{N' \Omega \nu}\right] = \frac{qa'V}{W_c X_L} - 1 \tag{34}$$

On substituting $-\frac{1}{\beta_L} = \frac{k}{W_c} \log \left[\left(\frac{dx}{dt}\right)_L \frac{1}{N' \Omega \nu}\right]$, (34) can be reduced to the form

$$\frac{1}{X_L} = \left[\frac{1}{\beta_L} \frac{W_c}{qa'V}\right]\left(\beta_L - T\right) \tag{35}$$

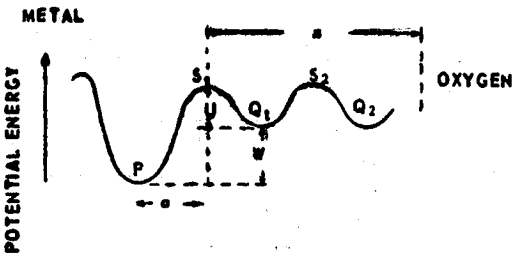

FIG. 8—Entry of cation from kink site at P into oxide layer

At temperature $T_c = \beta_L$, film grows to infinite thickness. At temperatures below the critical value, the film builds up rapidly at first, its rate of growth gradually slows down to a negligible value. (33) can be reduced to the form

$$\frac{1}{X} = K_{i1} - K_{i2} \cdot \log t \tag{36}$$

Roberts[15] has studied the oxidation of iron upto 920°C. Its rate of oxidation has been shown to follow the relationship

$$\frac{dx}{dt} = N' \nu \Omega \; P^{0\cdot 28} \; \exp \frac{-13000}{RT} \qquad (37)$$

where R is gas constant in calories/(temperature abs)

The low activation energy has been shown to arise from the effect of field due to chemisorbed oxygen. Electron diffraction[16] studies show that the oxide formed on iron sheet oxidized at 200°C is Fe_2O_3. Assuming $W_c = 20$k calories, $q = 3e$, $V \sim 1\cdot 8\, ev$, $X \sim 40A$, and $a' \sim 2\cdot 5$ A, the value of E_f is found to be 11·5k calories. This is in good agreement with experimental result [15] of 13·0k calories. The critical thickness X_l is found to be 6 to 12 monolayers of the oxide if $(dx/dt)_L$ is assumed equal to $(1/500)^{th}$ of monolayer per minute.

Mott & Cabrera's[11] mechanism has certain shortcomings. Strictly speaking this model is applicable to very thin films only. Reaction rate constant derived by them is independent of temperature. This is contrary to observation. Again factors such as orientation of the crystal face of the metal crystal, phase transformation in metals and magnetic changes at curie point have an influence on the rate of oxidation. To account for these observations Uhlig has assumed [13,14] that electron flow at the oxide/metal interface controls the rate of oxidation. The electron flow is supposed to be modified by space change in the oxide layer extending upto several thousand angstrom units. There may be two regions of space charge (*i*) region of uniform charge density next to the metal with thickness l, (*ii*) region of diffuse charge distribution beyond l upto total thickness L. The space charge regions are shown in Fig. 9*a* and 9*b*. The barrier heights are shown in Fig. 10*a* and 10*b*.

The regions of uniform and diffuse charge distributions in oxide film may show two distinct[14] logarithmic rates of oxidation. A suitable modification in charge distribution may lead to cubic rate. In neutral region linear or parabolic law may be obeyed depending upon limitation to reaction at the boundaries. Given below is a brief derivation of logarithmic law on the assumption that there is a uniform distribution of space charge in the oxide layer upto a critical thickness l.

In the space charge region Poisson's equation gives the relationship

$$d^2V/dx^2 = 4\pi ne/\epsilon \qquad (38)$$

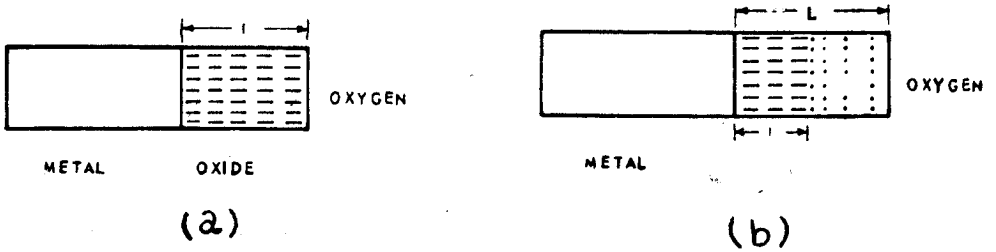

FIG. 9—Space change in oxide layer (*a*) uniform charge and (*b*) uniform and diffuse layers.

where ϵ is dielectric constant, e is the electronic charge, n is concentration of charge carriers and V is potential set up by chemisorbed layer of oxygen. Integration of (38) gives the relationship.

$$\frac{dV}{dx} = \frac{(4\ \pi\ nex)}{\epsilon} - \frac{(4\ \pi\ ne\ 1)}{\epsilon} \tag{39}$$

In (39) second term on the right hand side allows for the boundary conditions viz., $(dV/dx) \to 0$ at the metal/oxide interface as $x \to 1$. Further integration of (39) gives

$$V = \frac{4\ \pi\ ne}{\epsilon}\left(1x - \frac{x^2}{2}\right) - (\psi - v_o) \tag{40}$$

The last term gives the value of the potential $V = -(\psi - v_o)$ at the metal/oxide interface when $x \longrightarrow 0$. Here $e\psi$ is the energy required to remove an electron from the metal and place it on the oxide, and v_o is the electron affinity of the oxygen adsorbed on the oxide. It is well known that net current J across a potential barrier φ_o is given by the expression

$$J = A'\ e^{-e\ \phi_o/kT}\ (e^{eV'/kT} - 1) \tag{41}$$

where V' is applied potential and A' is a constant.

By making use of (40) and (41) it is possible to derive the relationship.

$$x = K_u\ \log\left(\frac{t}{\tau} + 1\right) \tag{42}$$

where

$$K_u = \frac{kT}{4\ \pi\ ne^2\ 1,}\quad \tau = \frac{\epsilon kT}{4\ \pi\ ne^2\ 1A}\ \exp\frac{e\ (\psi - v_o)}{kT}$$

or

$$\tau = \frac{K_u}{A}\ \exp\ \frac{e\ (\psi - v_o)}{kT}$$

The constant A is related to A'. The procedure outlined above can be extended to derive logarithmic expression for diffuse type of space charge.

The cubic law of growth of oxide layer can be deduced from special space charge distribution. It is assumed that density of charge carriers in the diffuse layer may be represented by means of the expression

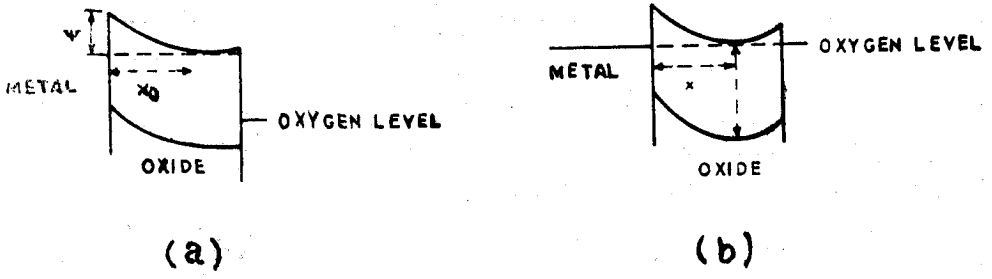

FIG. 10—(*a*) Energy barrier or electron trans fer x_o depth of space charge thickness and (*b*) energy barrier for electron transfer

$$n = n_o \exp\left(\frac{eV}{kT}\right) \tag{43}$$

The above expression is substituted in Poisson's equation (38). The solution of resulting equation is obtained by using the boundary conditions $dV/dx \longrightarrow 0$ as $x \to \infty$ and $V \to C_o$ as $x \to 0$. On these assumptions, it is possible to derive the cubic law

$$\left(x + x_o \exp\frac{-C_o e}{2kT}\right)^3 = \frac{3At}{x_o^{2/3}} + x_o^{1/3} \exp\frac{-3C_o e}{2kT}$$

where

$$x_o = \left(\frac{\epsilon kT}{2\pi n_o e^2}\right)^{1/2} \text{and } C_o = \left[-\frac{4\pi n e l L}{\epsilon} - (\psi - v_o)\right] \tag{44}$$

Mott & Cabrera[11] have derived the cubic law on the assumption that diffusion of cations/vacancies under the influence of the field set up by chemisorbed oxygen is the rate determining factor. The present discussion applies to movement of vacancies from oxide/gas interface to oxide/metal interface. The number of vacancies crossing unit area per unit time is $n_{\square} v_m F$ where $n_{\square}$ is concentration of vacancies, v_m is mobility and F is field strength. The rate of oxide growth is give by the expression

$$\frac{dx}{dt} = n_{\square} v_m \Omega F = \frac{n_{\square} U_m \Omega V}{X}$$

or

$$\frac{dx}{dt} = n_{\square}\left(\frac{D_e}{kT}\right) \Omega \frac{V}{x} \tag{45}$$

where D is diffusion coefficient. It may be assumed that number of vacancies $n_{\square}$ is proportional to concentration N_s of chemisorbed oxygen ions per unit area. (46) gives concentration of vacancies per unit area at the interface between oxide and oxygen

$$n_{\square} = \left(\frac{N_s}{a}\right) e^{-(W_{\square} + U_m)/kT} \tag{46}$$

where $W_{\square}$ and U_m are energies of activation for the formation and diffusion of vacancies respectively. The number of chemisorbed ions N_s per unit area is related to field strength F thus

$$N_s = F/4\pi e = \epsilon V/4\pi e x \tag{47}$$

Substitution of (47) in (46) and making use of the resultant relationship in (45) gives rate of oxide growth.

$$\frac{dx}{dt} = \frac{\epsilon V^2 D \Omega}{4\pi a kT}\left[e^{-(W_{\square} + U_m)/kT}\right]\frac{1}{x^2} \tag{48}$$

Integration of (48) gives the cubic law

$$x^3 = \left(\frac{3\epsilon V^2 D}{4\pi a kT}\right)\left[e^{-(W_{\square} + U_m)/kT}\right] t \tag{49}$$

Cabrera[17] has used this expression to explain the results obtained by Cambell and Thomas[18].

Field free Oxidation : Oxidation in field free region is controlled by diffusion of defects Wagner[19] has proposed a mechanism of oxidation which has been quite successful in assessing the rate of reaction. An accurate prediction of rate of oxidation requires information regarding nature of defects, their mobility v_m , transference number t and electrical conductivity σ. The reaction rate constant K_r is given by the expression

$$K_r = c \int_{\gamma_2}^{\gamma_1} \left[\frac{Z_1}{Z_2} D_1 + D_2 \right] d \log \gamma \qquad (50)$$

Here reaction rate constant may be defined as number of equivalents of the oxide formed per square cm per second, γ_1 and γ_2 are oxygen activities (or pressure) at metal/oxide and oxide/gas interfaces, Z_1 and Z_2 are valences of oxygen and metal ions, D_1 and D_2 are coefficients of diffusion of anions and cations and c is concentration of oxygen in equivalents per cm^3. One of the important factors which determines the composition and stability of the oxide is the ambient pressure. As for example under atmospheric pressure both FeO and Fe_3O_4 transform into Fe_2O_3. As soon as a protective film of Fe_2O_3 is formed both Fe_3O_4 and FeO oxides remain stable underneath. This is because equilibrium pressure of oxygen at the layers below the protective layer is low. Ambient pressure also affects the concentration of cation vacancies and holes in the oxide film.

Usually in oxide layer either interstitial cations and electrons move from metal/oxide interface into oxide layer or cation vacancies and holes move from oxide/gas interface into oxide. The space charge of moving cations or vacancies exerts a considerable influence on the movement of electrons and holes. The concentration and mobility of defects determine the rate of oxidation. Whenever the concentration of defects is low as in Al_2O_3, the rate of oxidation is low.

In thick, stable, coherent and dense films the rate of reaction is determined by concentration of defects at the two boundaries of oxide layer. If concentration of defects at both boundaries is independent of thickness, its gradient is inversely proportional to thickness. Under such conditions parabolic law holds good.

$$X^2 = 2At$$

Cabrera & Mott's method[11] of estimation of constant A in the parabolic growth law is given below. The discussion is based upon the assumption that interstitial cations and quasifree electrons are mobile. The currents arising from flow of interstitials J_i and electrons J_e are given by the expressions

$$J_i = - D_i \frac{\partial n_i}{\partial x} - F n_i V_i \qquad (52)$$

$$J_e = - D_e \frac{\partial n_e}{\partial x} + F n_e V_e \qquad (53)$$

where n, $v = D_e / kT$ are density of defects and mobility respectively. In steady state both J_i and J_e are equal and opposite. (52) and (53) may be used to eliminate F giving

$$J \left[\frac{1}{n_e v_e} + \frac{1}{n_i v_i} \right] = - \frac{kT}{e} \frac{\partial}{\partial x} \log (n_i n_e) \qquad (54)$$

where J is number of atom (electrons, ions) crossing per unit area per unit time.

If it is assumed that $n_i\ (x) = n_e\ (x) = n$, and $v_e >> v_i$, (54) may be expressed in the form

$$J = -2D_i \frac{\partial n}{\partial x} \tag{55}$$

Integration of (55) gives the expression

$$Jx = 2\ D_i\ [\ n\ (o) - n\ (x)\ ] \tag{56}$$

The rate of growth of the film is given by the expression

$$\frac{dx}{dt} = 2\ D_i\ \Omega \left[\ n\ (o) - n\ (x)\ \right] \frac{1}{x} \tag{57}$$

where x is film thickness and Ω is volume of oxide per metal ion Here subscripts (o) and (x) refer to metal/oxide and oxide/gas interfaces respectively. Integration of (57) gives the parabolic law. It is proposed to discuss a few typical cases of oxidation of metal involving diffusion in field free region.

Oxidation of copper—On oxidation of pure copper in air a composite layer of Cu_2O and $Cu\,O$ is formed. 90 per cent of the volume of oxide in this layer consists of Cu_2O. Remaining 10 per cent of the volume of the layer on the top consists of $Cu\,O$. It is the rate of diffusion of Cu^+ ions through Cu_2O which controls the rate of oxidation of copper. The pressure of oxygen at the interface of Cu_2O/CuO may be dissociation pressure of CuO. The constancy of this pressure helps to maintain the concentration of cation vacancies at this interface constant. The metal/oxide interface has no vacancies. In view of these two boundary conditions, ambient pressure of oxygen has no appreciable effect on the rate of oxidation of copper in air.

At a low partial pressure of oxygen in H_2O/H_2 or CO_2/CO mixture, copper is oxidized to pure Cu_2O. The oxygen absorbed on surface of Cu_2O is transformed into O^{2-}ions by accepting electrons from Cu_2O layer. Holes are injected into the lattice. The concentration of cation vacancies $C_{\square_{cu}^+}$ and holes C_h are dependent upon oxygen pressure as shown below:

$$\tfrac{1}{2}\ O_2 \rightleftharpoons O^{=}\ (\text{matrix}) + 2\square_{cu}^{+} + 2h^+ \tag{58}$$

Law of mass action gives the relationship

$$\frac{(C_{\square_{cu}^+})^2\ (C_h^+)^2}{[\ P.\ (O_2)\ ]^{\frac{1}{2}}} = \text{Constant} \tag{59}$$

By making use of the condition of electroneutrality $C_h^+ = C_{cu}^+$, (59) can be reduced to the form

$$C_h{}^+ = \text{constant}\ \ [\ P\ (O_2)\ ]^{1/8} \tag{60}$$

The electrical conductivity σ is proportional to $C_h{}^+$ and according to (60) it is proportional to $[\ P\ (O_2)\ ]^{1/8}$. Experimental work[20] gives $[\ P(O_2)\ ]^{1/7}$ which is fairly in good agreement with theory. In oxidation of copper mobility of $v_{\square_{cu}}$ is a rate determining step. (50) can be put into the form

$$K_r = \text{constant}\ (\ 1 + Z_{cu}{}^+)\ v_{\square_{cu}}\ kT\ (\sqrt[7]{(P.O_2)_2} - \sqrt[7]{(P.O_2)_1}) \tag{61}$$

The observed[21] and calculated values of K_r are in good agreement.

Oxidation of nickel[22] *involving p type oxide*—An oxygen molecule may be adsorbed at a vacant anion site on nickel oxide and may give rise to nickel ion vacancy and two positive holes

$$\tfrac{1}{2}\, O_2 \rightleftharpoons O^{2-} + \square_{Ni}{}^{+} + 2\, h^{+} \tag{62}$$

Electrical neutrality gives the condition

$$\tfrac{1}{2}\, n_h = n_{\square} \tag{63}$$

where n is concentration of defects. Law of mass action leads to the expression

$$\frac{\left(\frac{n_h}{N}\right)\left(\frac{n_{\square}}{N}\right)}{(P_{O_2})^{1/2}} = e^{-\triangle G/kT} \tag{64}$$

where $\triangle G = H + T \triangle S$ is change in free energy, $\triangle H_f$ is heat of formation and $\triangle S_f$ is entropy of formation of cation vacancy, N is Avogadro's number, (64) can be put into the form

$$n_{\square} = \frac{N}{(4)^{1/3}}\, (P_{O_2})^{1/6} \exp \frac{-\triangle G}{kT} \tag{65}$$

The constant in parabolic law has the form

$$A_{Ni} = 2\, \Omega\, D\, (n_{1_{\square}} - x_{2_{\square}}) \tag{66}$$

where $n_{1_{\square}}$ and $n_{2_{\square}}$ are concentrations of vacancies per cm^3 at oxide/gas and oxide/metal interfaces respectively. Since $n_2 \sim O$, reaction constant can be put into the form

$$A_{Ni} = 2\, \Omega\, DN\, (P_{O_2})^{1/6} (\tfrac{1}{4})^{1/3} \exp \frac{-\triangle G}{3\, kT} \tag{67}$$

Zener's[22] theory gives

$$D = \theta\, a^2\, \nu \exp \frac{-\triangle G^X}{kT} \tag{68}$$

where θ is a constant characterizing nature of jumps. Substitution of (67) in (68) gives

$$A_{Ni} = 2\, \theta\, a^2\, \nu\, \Omega\, N\, (P_{O_2})^{1/6}\, (\tfrac{1}{4})^{1/3} \exp \frac{-\left(\frac{\triangle G}{3} + \triangle G^X\right)}{kT}$$

where $\triangle G^X = \triangle H^X + T \triangle S^X$ is change in free energy for diffusion. The value of $\triangle S^X$ derived from (69) compares favourably with experimental results[23].

Oxidation of zirconium—The study of oxidation of zirconium in CO_2 is important in reactor technology. This gas is used as a coolant and zirconium as canning material. The reactions on zirconium surface may be written as

$$CO_2\,(g) \rightleftharpoons CO_2\,(a) \qquad \text{fast} \tag{70}$$

$$CO_2 + 2e \rightleftharpoons CO\,(g) + O^{2-}\,(a) \qquad \text{slow} \tag{71}$$

$$O^{2-}(a) \rightleftharpoons \overline{O}\ (\text{Oxide}) \qquad \text{fast} \tag{72}$$

or

$$Zr + 2\, CO_2 \rightleftharpoons ZrO_2 + 2\, CO \tag{73}$$

The values of migration and activation energy are $\triangle U_m = 17$, $\left(\triangle U_m + \frac{\triangle H_f}{2} \right) =$ 65k calories/mole in the temperature ranges of 200—350°C and 600—700°C respectively; $\triangle U_m$ is energy for migration and $\triangle H_f$ is the energy for formation of Frenkel anion defects.

Below 700°C, the film formed at the oxygen partial pressure of 10^{-1} mm is protective. Between 630 to 730°C the dependence of oxidation rate r on pressure is given by the relationship

$$(r_1/r_2) = (P_1/P_2)^{-0.3} \tag{74}$$

The negative pressure index is compatible[24] with mechanism involving anion vacancies

$$(\overline{\overline{O}}) \rightleftharpoons \square\overline{\overline{O}} + \bar{e} + \tfrac{1}{2} O_2 \tag{75}$$

A value of about 95k calories per mole is estimated for heat of formation of Frenkel defect (anion type) in zirconium oxide.

Oxidation of Niobium—Oxidation of niobium has been studied by Kofstad & Espevik[25] in temperature range of 1200°—1700°C and pressure range of 2×10^{-4} to 0·5 Torr. The oxidation occurs in three main stages (*i*) linear oxidation, (*ii*) parabolic stage and (*iii*) linear growth. The initial stage involves dissolution of oxygen in the metal. The oxidation is governed by rate of chemisorption on the metal surface

$$O_2\ (g) \underset{k_{-1}}{\overset{k_1}{\rightleftharpoons}} O_2\ (a) \tag{76}$$

$$O_2\ (a) + 2 \text{ sites} \rightleftharpoons 2\,\bar{O}\,(a) \tag{77}$$

X-ray studies indicate that parabolic oxidation involves protective NbO_2 layer which is compact and shows excellent adhesion. The square root pressure dependence of reaction rate $K_p \propto (Po_2)^{1/2}$ rules out existence of mobile oxygen vacancies but suggests the presence of interstitial oxygen

$$\tfrac{1}{2} O_2\ (g) \rightleftharpoons \overset{z-}{O_1} + zh^+ \tag{78}$$

The activation energy in the parabolic range is 44 k calories. At higher oxygen pressure NbO_2 is oxidized to Nb_2O_5 which is porous and has no protective property. In this range the growth rate is also linear and the mechanism of reaction may be similar to initial stage. At temperatures above 1500°C, Nb_2O_5 becomes liquid and is not protective.

At high temperature and high oxygen pressure the equilibrium between the oxide and oxygen gas may be represented by means of the equation

$$Nb_2O_5 \rightleftharpoons Nb_2O_{5-\chi} + \frac{\chi}{2} O_2\ (g) \tag{79}$$

The value of χ is calculated from changes in weight[26]. The equilibrium affecting concentration of defects may be represented by means of the equations

$$\overline{\overline{O}} \rightleftharpoons \square\overline{\overline{}}_{Nb} + \tfrac{1}{2} O_2 \tag{80}$$

$$\overline{\overline{O}} \rightleftharpoons \square_{\overline{Nb}} + e + \tfrac{1}{2} O_2 \tag{81}$$

$$\overline{\overline{O}} \rightleftharpoons \square_{Nb} + 2e + \tfrac{1}{2} O_2 \tag{82}$$

The energies for ionization of electrons entrapped by vacancies in (80) and (81) are 0·2 and 0·9 ev respectively. The condition of electronegativity gives

$$C_{\square_{Nb}^{-}} = C_e \text{ and } C_{\square_{Nb}} = 2\ C_e$$

On application of law of mass action, it is found that concentration of vacancies is given by the expression

$$C_{\square_{Nb}} = \text{Constant} \left[P_{O_2} \right]^{-1/4} \tag{83}$$

$$C_{\square_{Nb}} = \text{Constant} \left[P_{O_2} \right]^{-1/6} \tag{84}$$

Electronic conductivity[27] is found to vary as $P^{-\frac{1}{4\cdot2}}$ near stoichiometry ($P_{O_2} = \cdot001$ to one atmosphere) and as $P^{-1/6}$ in the low pressure. It appears that oxygen vacancies are singly ionized near stoichiometry and doubly ionized at large vacancy concentrations of defects. The high degree of ionization at large deviations[28] from stoichiometry can be explained by assuming overlap of defect orbitals which causes Fermi level to move upwards.

Oxidation of zinc—zinc is one of the reactive metals. At temperatures below 375°C its oxidation occurs in accordance with logarithmic law. At temperatures above 375°C oxidation follows a parabolic law. It is movement of interstitial Zn^+ ions which controls the rate of reaction. Equilibrium between various defects may be represented by means of the expression

$$\tfrac{1}{2}\ O_2 + e + Zn_i^+ \rightleftharpoons ZnO \text{ (matrix)} \tag{86}$$

Condition of electro-neutrality yields $C_{zn}^{+} = C_e$.

Application of law of mass action gives the relationship

$$C_{Zn}^{+}\ C_e \left[P_{(O_2)} \right]^{1/2} = \text{constant} \tag{86}$$

$$\text{or } (C)^2 \left[P_{(O_2)} \right]^{1/2} = \text{constant}$$

$$\text{or } C_e = (\text{constant}) \left[P_{(O_2)} \right]^{-1/4} \tag{87}$$

(87) shows that conductivity is proportional to $[P_{(O_2)}]^{-1/4}$ which is in agreement with experimental[29] results.

Oxide layer at metal/oxide interface is saturated with interstitial Zn^+ ions and electrons and the layer at oxide/gas interface has negligible amount of interstitials. The concentrations of interstitials at both boundaries are almost independent of ambient pressure. Growth of zinc oxide layer follows a parabolic law and is dependent upon diffusion of Zn^+ ions. The rate of diffusion of zinc in ZnO under an atmosphere of zinc vapours is given by the expression $D = 5{\cdot}3 \times 10^{-4} \exp \frac{-0{\cdot}55\ ev}{kT}$ cm²/sec. The variation with temperature of solubility of zinc in zinc oxide is given by the expression

$$n = 3{\cdot}4 \; x \; 10^{20} \exp \frac{-0{\cdot}65 \; ev}{kT} \quad \text{atoms/cm}^2 \tag{88}$$

The calculated[30] energy of activation for oxidation is found to be 1·20 ev. This value compares favourably with experimental [31,22] value of 1·08 ev. The small difference between the two may be due to quenching process involved in Thomas' solubility determination[30] and possibility of anisotropic diffusion. On disolution of zinc in zinc oxide there is an increase in entropy equal to 8·7 cal g atom^{-1} degree^{-1}. This value gives vibrational frequency of $1{\cdot}1 \times 10^{13}$ which is nearly equal to optical mode of vibration of zinc oxide. Impurities influence the rate of oxidation. Presence of 0·1 atom per cent of aluminium in zinc depresses the rate by a factor 10^2. Lithium has a reverse effect though to a lesser extent. Both these elements enter into zinc oxide substitutionally. Addition of aluminium may increase concentration of electrons in zinc oxide. The equilibrium between defects can be represented by means of the equation

$$Al_2O_3 \rightleftharpoons 2 \, \overset{3+}{Al}_{Zn} + 2 \, e + \tfrac{1}{2} \, O_2 + \bar{O} \text{ (matrix)} \tag{89}$$

where $\overset{3+}{Al}_{Zn}$ denotes aluminium ion present at site of $\overset{2+}{Zn}$. Condition of electroneutrality gives the relationship

$$C_e = C_{Zn_i} + C_{Al_{Zn}} \tag{90}$$

where C_{Al} denotes concentration of aluminium atoms present at zinc sites. Application of law of mass action gives the relationship

$$C_e \; C^{+}_{Zn_i} = \text{constant} \tag{91}$$

$$C^{\circ}_e \; C^{\circ +}_{Zn_i} = \text{constant} \tag{92}$$

Here superscript o denotes concentration of defects in pure oxide. Equations (90), (91) and (92) can be combined to yield the relationship

$$\left(\frac{k_{Zn}}{k^{\circ}_{Zn}} \right)_{Al} = 1 - \frac{C^{+}_{Zn_i} \; C_{Al}}{C^{\circ}_{Zn_i}} \tag{93}$$

where k_{zn} and k°_{zn} are reaction rate constants for doped and pure zinc oxide respectively. (93) indicates that incorporation of aluminium in zinc reduces rate of oxidation. This result is in conformity with experimental data.

Equilibrium between defects produced on incorporation of lithium into zinc oxide can be represented by means of the equation

$$\tfrac{1}{2} \, O_2 + 2 \, \bar{e} + Li_2 \, O \rightleftharpoons 2 \, Li_{zn}{}^{+} + 2 \, \bar{\bar{O}} \tag{94}$$

Condition of electroneutrality gives the relationship

$$C_{Zn_i}{}^{+} = C_e + C_{Li} \tag{95}$$

Application of law of mass action yields the expression

$$C_{Zn_i}{}^{+} = C_e = \text{constant} \tag{96}$$

A relationship similar to (96) holds good for pure zinc oxide. By making use of the expressions (95) and (96) it is possible to derive the result

$$\left(\frac{k_{zn}}{k^{\circ}_{zn}} \right)_{Li} = 1 + C_{Li} \; C^{+}_{Zn_i} \tag{97}$$

This expression shows that doping of zinc oxide with lithium increases rate of oxidation of zinc. This result again agrees with experimental observations.

The addition [32] of thallium to zinc has an interesting effect on its rate of oxidation. The rate is higher at 0·1 atom % of thallium than in pure zinc. The rate falls below that in pure zinc at 0·5 atom % of thallium. A possible explanation is the change in valency of thallium. It may be monovalent at lower concentration. At higher concentration it may exist in trivalent form. Resistance towards oxidation of nichrome (80% *Ni*—20% *Cr*) may arise from formation of a layer of spinel $Ni\,Cr_2O_4$ on the surface. Coating of niobium with zinc affords protection upto 1000°C. Zinc forms a complex $NbZn_3$ on the surface. On oxidation zinc oxide is formed on surface which plugs up openings in porous niobium oxide and prevents further oxidation.

Oxidation of Silicon—In planar transistor technology silicon is covered by a surface layer of silicon dioxide. This glassy surface effectively blocks the passage of impurity atoms. Atalla, Tannenbaum & Scheibner [33] have studied the oxidation of silicon in dry and wet oxygen by making use of micro-balance technique. The oxidation process follows the following parabolic laws :

$$O_2 : X^2 = 8.4 \times 10^{10}\; p^{4/5}\; t\; e^{(-1\cdot4\, ev/kT)} \tag{98}$$

$$H_2O : X^2 = 2\,54 \times 10^{13}\; p^{8/5}\; t\; e^{(-1\cdot7\, ev/kT)} \tag{99}$$

The thermally produced oxide is homogenous and amorphous. It has a dielectric constant of 4 and has a resistivity of 10^{16} ohm-cm. Ainger [34] has studied the devitrification of the oxide above 1300°C by means of electron microscope and electron diffraction. This oxide exhibits a cubic structure with cell size 8·16A which does not correspond to normal structure of silica.

Deal[35] has extended these investigations. He has studied the kinetics of oxidation of silicon in dry oxygen, wet oxygen and in steam. He has come to the conclusion that wet oxygen process produces silicon dioxide with best protective characteristics which include density, dielectric strength, masking ability and freedom from defects. Films produced by dry oxidation contain appreciable concentration of point defects. The control of oxidation in steam oxidation is not easy. Oxidation above 1000°C follows a parabolic rate law. Below 1000°C the oxidation changes to a combination of parabolic and linear laws. During parabolic growth diffusion plays a dominant role. In the linear region the oxidation is controlled by reaction at the interface of silicon/oxide. In view of this behaviour the activation energy determined in the region 1000°—1200°C is only meaningful. For diffusion controlled mechanism Deal's values of activation energy in dry oxygen, wet oxygen and steam are 30·2, 20·8 and 19·9k calories per mole respectively. These values are lower than those of Atalla *et al*[33].

With a view to locate the diffusing species Ligenza and Spitzer [36] have investigated the infra-red spectra of layers of SiO_2 produced by oxidation of silicon in succession in the gas containing oxygen isotopes O^{16} and O^{18}. The yhave observed that absorption bands at 9·25 and 21·9 μ in SiO_2^{16} shift to 9·6 and 22·6 microns in SiO_2^{18}. Based upon the infra-red shifts of these bands, they have suggested that the atmosphere used in last stage of oxidation has a profound effect on the entire film. There is a rapid exchange of isotopes. The isotope last used penetrates the entire film. To explain this observation it has been assumed that a species of oxygen diffuses by isotopic exchange to the silicon/silica interface.

Deal & Sklar [37] have investigated the effect of doping on rate of oxidation. They have observed that heavy doping of silicon with impurities like boron increases the rate of oxidation. This effect may be due to increase in imperfections in oxide film. On a substrate, pyrolytic [38] film of pure silicon dioxide can be obtained from thermal decomposition of tetra-ethoxy silane in the temperature range of 625°—900°C. Densification of these films can be achieved by heating at 800°C in steam which is more effective than dry atmosphere. The films produced by various methods can be assessed [39] by studying refractive index, etch rate, infra-red spectra stcichiometry, passivation efficiency and thermal densification studies. The pyrolytic films shows higher rate of etching. Anodized[33] film produced by oxidation in a bath of ·05M KNO_3 in methyl acetamide shows presence of bond strain as revealed by width and position of 1074 cm^{-1} peak in the infrared.

The oxidation rate is strongly dependent on orientation. Ligenza [40] has predicted that in oxidation under high pressure of steam, rate of reaction on (100) surface should be less than on (110) or (111) face. Atomic arrangement on (100) face of silicon is shown in Fig. 11(*a*) and the shape of band near the surface of pure silicon is given in Fig. 11(*b*). This surface has fewer bonds or reaction sites. Experimental work of Deal [35] shows that very little difference is observed in the rate of oxidation at different faces above 1200°C. However the rate of oxidation below 1000°C on (100) face in wet oxygen is much lower than that of (111) and (110) faces. The rate of epitaxial growth follows a similar behaviour. The observed rate of deposition at slow speed versus misorientation from (111) plane is shown[40] in Fig. 12. The epitaxial growth is lowest on accurately oriented (111) substrate. It increases as the degree of misorientation from (111) plane increases. (110) face possesses the highest rate of deposition. The rate of deposition from a mixture of $SiCl_4$ and H_2 depends upon two terms[41]. The first term is the rate of transfer of silicon towards the interface as $SiCl_4$, the second term contains the thermodynamic equilibrium constant. The rate of deposition passes through a maximum as the concentration of $SiCl_4$ is increased.

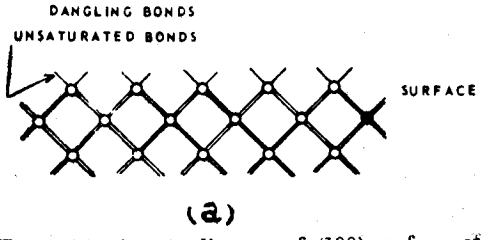

FIG. 11(*a*)—Atomic diagram of (100) surface of silicon

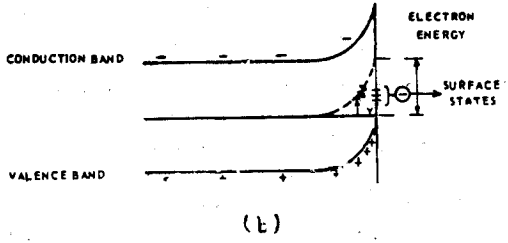

FIG. 11 (*b*)—Band bending near the surface of an atomically clean intrinsic materials

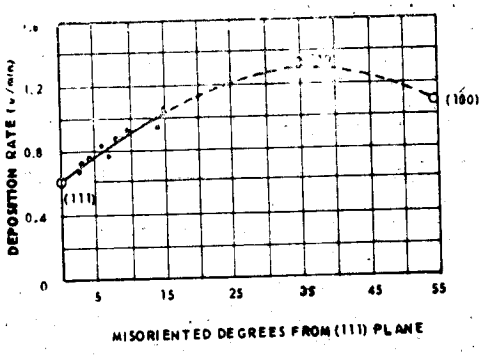

FIG. 12—Deposition rate on substrate of silicon

Anodic Oxidation—Compact oxide films can be produced by anodic oxidation of silicon, tantalum and aluminium. Tantalum oxide films are receiving a good deal of attention for production of miniature capacitors. Tantalum can be anodically oxidized in dilute sulphuric acid. Interpretation of kinetics of anodic oxidation depends upon movement of metallic cations as shown by Vermilyea[42], Amsel & Samuel[43]. Calvert & Draper [44] find that oxide films on tantalum are amorphous at all concentrations of sulphuric acid. On heating, the films crystallize to pentoxide. Even in amorphous films there is local order. Ta^{5+} ions are surrounded by O^{2-} ions and *vice versa*. The local non-stoichiometry can still be described in terms of vacancies and interstitials. De-wald [45] has given the following relationship between strength of the current and electric field F :

$$F = \left[\frac{2kT}{(a_3 + a_1)} \log \left(\frac{\alpha j}{\nu q}\right)\right] + \frac{U_3 + U_1}{(a_3 + a_1) q} \qquad (100)$$

where U and a are activation parameters of ion-vacancy pairs. Subscripts '3' and '1' indicate formation and migration of defects respectively, α is a constant, and q is charge on moving ion. Experimental results [46] indicate $a_1 = 3{\cdot}15A$, $a_3 = 1{\cdot}50\ A°$, $U_3 = 1{\cdot}21$ and $U_1 = 2{\cdot}22$ *ev*. The Tafel slope is given by the expression

$$\frac{\partial F}{\partial \log J} = \frac{2\ kT}{q\ (a_1 + a_3)} \qquad (101)$$

Amsel and Samuel[43] have investigated the mechanism of anodic oxidation of aluminium by studying the sharp resonances of nuclear reactions O^{18} (p, α) N^{15} and Al^{27} (p, γ) Si^{28}. For these studies a composite film containing O^{18} and O^{16} in successive layers has been produced by anodic oxidation in electrolytes containing these isotopes. The resonance shifts in stripped films have been measured. The examination has been carried on the film from metal side and from electrolyte side. The observed shifts indicate that order of oxidation is conserved in the film. On the basis of these results it has been proposed that oxygen sub-lattice remains stationary during oxidation. The migration of cations involves both vacancy diffusion and interstitialcy mechanism. Recent investigations based upon study of α and β spectroscopy[47] indicate that in Al_2O_3 and Ta_2O_5 both cations and anions migrate[48]. In anodic oxidation of silicon[49] it has been observed that presence of Cl' and F' ions in the electrolyte has a favourble effect on rate of oxidation. It appears that Cl' and F' ions are incorporated at oxygen sites and Si^{4+} vacancies are created. The presence of these vacancies helps in migration of silicon ions.

Epitaxial growth

Orientation of a film of the new phase on anisotropic substrate is called epitaxy. A pseudomorphic layer of the new phase grows on the substrate if certain conditions are satisfied. If a and b are lattice spacings of the substrate and new phase, the misfit may be defined as $M = \left(\frac{b}{a} - 1\right)$. Van der Merve[50] find that if degree of misfit is less than 15% the film takes up the lattice parameters of the substrate. If misfit is greater than 15% it may take up its own unstrained lattice parameters. On formation of the successive layers of the new phase, the force constant of the film becomes large. There is a tendency for the film to break away from the substrate. It may be mentioned that compressive strength of a thin film is much larger than that of the bulk material. The break in film occurs by slip or recrystallization. On rupture each island of the film rotates about a line perpendicular to the surface. The two dimensional order disappears.

Formation of epitaxial oxide layer on the metal surface may be followed by electron diffraction. The change in azimuth angle of the sample with respect to beam direction may or may not change the diffraction pattern. Appearance of an altered pattern with change in azimuth angle implies two degree oriented growth. A uniformity in pattern indicates one degree oriented growth. Goswami and Trehan[51] have followed oxidation of copper on (110), (100) and (111) faces. They have observed that Cu_2O film having {110} orientation and two degree order is formed at 200°C on (110) face of copper. Below 200°C as film thickness increases, crystals of cupric oxide having {110} and two dimensional order appear on the layer of Cu_2O. The epitaxy of underlying Cu_2O remains unchanged.

Oxidation of copper at 160°C on (100) face gives (111) oriented crystals of Cu_2O which give repeat diffraction pattern at every 15° azimuth rotation. The <110> axes of the Cu_2O may align along the face edges and face diagonals. On the basis of this assumption it is easy to explain the repeated pattern at every 15 rotation. On (111) face of copper at 160°C crystals of Cu_2O with (111) orientation are formed. These crystals give same patterns at azimuth angles of 0°,30°, and 180° relative to copper lattice. It appears that in addition to (111) orientation crystals of Cu_2O with <211> direction parallel to <110> direction of copper are formed. Such an arrangement explains the similarity of pattern at azimuth rotation of 0° and 30° C. {111} twinning may be responsible for repeat pattern observed at azimuth rotation of 180°. Twinning provides relief of stress which is generated at metal/oxide interface due to misfit. During oxidation at 300°C the CuO oxide film formed as epitaxial layer on (110) face undergoes a change. The (111) oriented CuO film loses two dimensional order and retains only one degree orientation. The film thickness at this stage may be 1260A. Similar phenomena are observed on (110) and (111) faces. Initially two degree oriented CuO crystals are formed at 250°—300° C over epitaxially grown Cu_2O layer. As the film becomes thick one degree (111) oriented CuO crystals are formed. Rhodin[52] has shown that of the most commonly occuring planes on copper surface, the (110) plane is most readily oxidized and the (111) plane the least.

Singh & Acharya have studied the formation of Bi_2S_3 on (0001) face of bismuth by the action of sulphur. Electron diffraction patterns of freshly cleaved and treated surfaces are shown in Fig. 13*a* and 13*b* respectively. The treatment consists in cleaving the crystal, allowing it to react with S for 24 hours at room temperature. The pattern given in Fig. 13*a* contains spacing of 100 planes of bismuth. The bismuth sulphide pattern in Fig. 13*b*

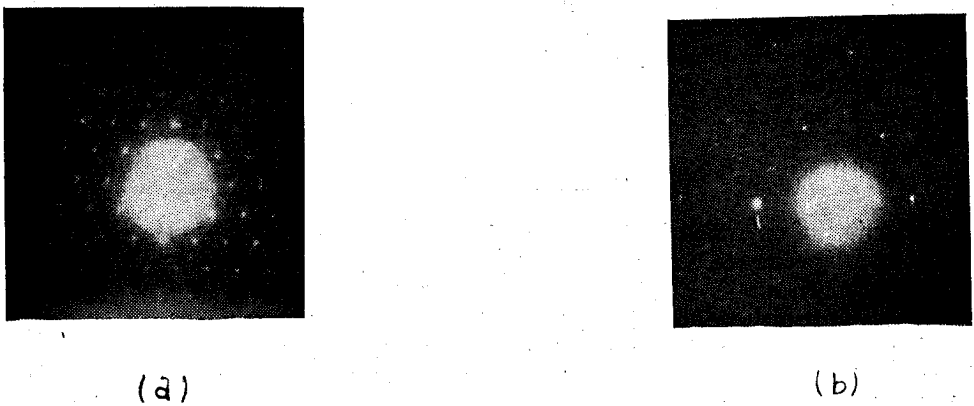

FIG 13—(*a*) Electron diffraction pattern of bismuth (0001) face and (*b*) electron diffraction pattern of (0001) face of bismuth exposed to sulphur for 24 hours

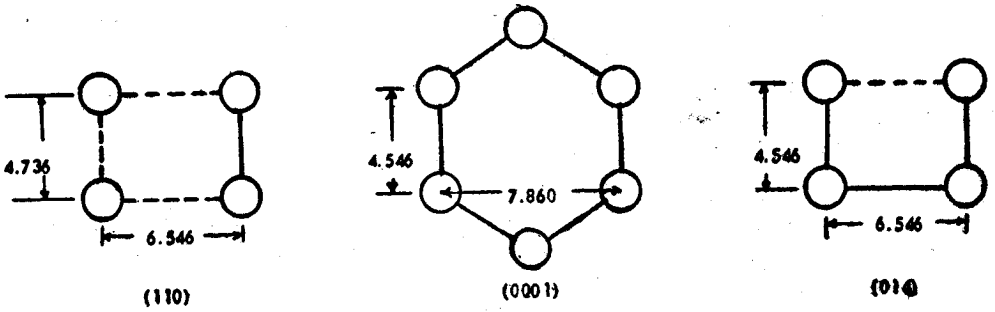

(a)

FIG 14 (*a*)—Atomic arrangement in bismuth

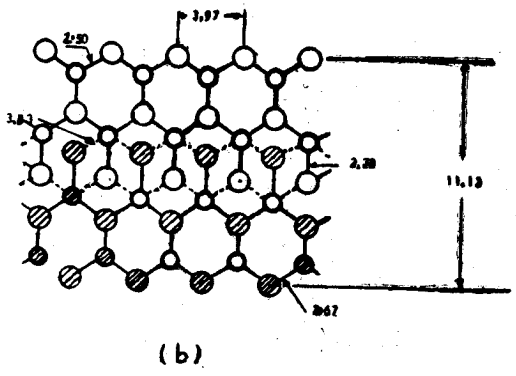

(b)

FIG 14 (*b*)—The double Bi_2S_3 chains in (diagrammatic).—The larger circles represents atoms. All the atoms of one chain are shaded and those of second chains are shown as broken lines

shows spacings of (503) and (500) planes which fit into unit cell size suggested by Hofman[53]. It is suggested that (010) plan of Bi_2S_3 is parallel to (0001) face of bismuth shown in Fig. 14*a*. A crystal of bismuth sulphide consists of a pair of chains shown in Fig. 14*b* which extend to infinity in one direction. Each $(Bi)_{11}$ atom is at a distance of 2·5A from three sulphur atoms and each $(Bi)_{11}$ atom is at a distance of 2·38A from one sulphur atom and 2·83A from other two atoms. The chains lie flat on (0001) face of bismuth.

CONCLUSION

The mechanism of oxidation in field free region of some metals is fairly clear. There is a need for investigations on nature of defects and mechanism of their migration. In case of reactions which are limited by speed at one of the interfaces there is a need for spectroscopic studies which will provide data required in calculation of partition functions of the reacting species. The position regarding the mechanism of oxidation in space charge region is not satisfactory. Quantitative information regarding the height of potential barrier, electronic structure of oxide layer and process of formation and migration of defects within the oxide layer is required.

REFERENCES

1. GERMER, L.H. & MACRAE, A.U., *J. Chem. Phys.*, **37** (1962), 1382.
2. LANDER, J.J. & MORRISON, J., *J. Appl. Phys.*, **34** (1963), 1403.
   —— , *J. Chem.* Phys., **37** (1962), 729.
3. BARRY, T. I. & STONE, S., *Proc. Roy. Soc.*, 285 (1960), **124.**
4. BEVAN and ANDERSON, *Dicsussion Faraday Soc.*, **8** (1950); 238.
5. MARCELLINI, RANE & TEICHNER, *2nd. Int. Congr. Catalyst.*, Paris, 1960.
6. WINTER, E. R. S., *J. Chem. Soc.*, (1954) 1522, (1955) 3824.
7. ——, *Discussion Faraday Soc.*, **28** (1959), 183.
8. CHARMAN, H.B., DELL, R. M. & TEALE, S.S., *Trans. Faraday Soc.*, **59** (1963), 453.
9. MOTT, N.F.,GURNEY, R.W., "Electronic Processes in ionic crystals" (Oxford University Press, (1948)), p 260
10. FREEMAN, E. S. & CAMPBELL, C., *Trans. Faraday Soc.*, **59** (1963), 165.
11. CABRERA, N. & MOTT, N.F., Reports on Progress of Physics, **12** (1948), 163.
12. UHLIG, H.H., *Acta Metallurgica*, **4** (1956), 540.
13. UHLIG, H., PICKETT, J. & MACNAIRN, J., *ibid*, **7** (1959), 111.
14. MITROFANOV, OV, Soviet Physics—Crystallography 8, No. 2, Trans (1963), p. 229.
15. ROBERTS WYN, *Trans. Faraday Soc.*, **57** (1961), 99.
16. VERNON, W. H. J., CALNAN, E. A., CLEWS C. J. B. & NURSE, T. J., *Proc., Roy. Soc.*, **216A** (1953), 375.
17. CABRERA, N., *Phil. Mag.*, **40** (1949), 175.
18. CAMPBELL, W.E. & THOMAS, U.B., *Trans. Electrochem. Soc.*, **91** (1947), 345.
19. WAGNER, *Z. Physik, Chem.*, **21B** (1933), 25.
20. DUNWALD, H. & WAGNER, C., *Z. Phys. Chem.*, **17B** (1932), 467.
21. WAGNER, C. & GRUENEWALD, K., *Z. Phys. Chem.*, **40B** (1938), 455.
22. ZENER, C., *J. Appl. Phys.*, **22** (1951), 372.
23. GULBRANSEN, E.A., Proc. Gottenberg Conference on Solid State Reactions, 1952.
24. QINN, C.M., ROBERTS, M.W., *Trans. Faraday Soc.*, **159** (1963), 985.
25. KOFSTAD, P. & ESPEVIK, S., *J. Electrochem. Soc.*, **112** (1965), 153.
26. KOFSTAD, P. & ANDERSON, P.B., *J. Phys. Chem. Solids*, **21** (1961), 280.
27. KOFSTAD, P., *ibid.*, **23** (1962), 1571.
28. GREENER, E. H. & HIRTHE, W. M., *J. Electrochem. Soc.*, **109** (1962), 600.
29. BAUMBACH VOH, H.H. & WAGNER, C., *Z. Phys. Chem.*, **22** (1933), 199.
30. Thomas, D.G., *J. Phys. Chem. Solids*, **3** (1957), 229.
31. COPE, J. O., *Trans. Faraday Soc.*, **57** (1961), 493.
32. GENSCH, C.H. & HAUFFE, K. *Z. Physik Chem.*, **195** (1950), 386., *Z. Physik Chem.*, **196** (1950), 427.
33. Atalla, M.M., TANNENBAUM, E. & SHEIBNER, E. J., *J. Bell System Technical Journal*, **38** (1959), 749; **39** (1960), 933.
34. AINGER, F.W., *J. Materials Sciences*, **1** (1966), 1.
35. DEAL, B.E., *J. Electrochem, Soc.*, **110** (1963), 527.
36. LIGENZA, J.R. & SPITZER, W.G., *J. Phys. Chem. Solids*, **14** (1960), 131.
37. DEAL, B.E. & SKLAR, M., *J. Electrochem. Soc.*, **112** (1965), 430.
38. SHEPPERD, W. H., *ibid.*, **112** (1965), 988.
39. PLISKIN, W.A. & LEHMAN, H.S., *ibid.*, **112** (1965), 1013.
40. LIGENZA, J.R., *J. Phys. Chem.*, **65** (1961), 2011.
41. TUNG, S.K., *J. Electrochem. Soc.*, **112** (1965), 436.

42. VERIMLYEA, D.A., *Acta. Met.*, **4** (1954), 482.
43. AMSEL, G. & SAMUEL, D., *J. Phys. Chem. Solids*, **23** (1962), 1707.
44. CALVERT, L. D. & DRAPER, P. H. G., *Can. J. Chem.*, **40** (1962), 1943.
45. DEWALD, *J. Phys. Chem. Solids*, **2** (1957), 55.
46. DRAPER, P.H.G. & JACOBS, P.W.M., *Trans. Faraday Soc.*, **59** (1963), 2888.
47. DAVIES, J.A. *J., Electrochem. Soc.*, **109** (1962), 999, 1082; **110** (1963), 849.
48. HOAR, T. P. & MOTT, N.F., *J. Phys. Chem. Solids*, **9** (1959), 97.
49. SCHMIDT, P.F. & MICHEL, W., *J. Electrochem. Soc.*, **104** (1957), 230.
50. MERWE VAN, DER, *Discussion Faraday Soc.*, **5** (1949), 208.
51. GOSWAMI, A. & TREHAN, T. N., *Trans. Faraday Soc.*, **52** (1956), 358; **54** (1958), 1703.
52. RHODIN, T. N., *J. Amer Chem. Soc.*, **73** (1951), 3143.
53. HOFMAN, W., *Z. Krist.*, **86** (1933), 225.